

PHYSICS OF THE MERGING CLUSTERS CYGNUS A, A3667, AND A2065

MAXIM MARKEVITCH^{1,2}, CRAIG L. SARAZIN³, AND ALEXEY VIKHLININ^{1,2}

ApJ in press; astro-ph/9812005 v2

ABSTRACT

We present *ASCA* gas temperature maps of the nearby merging galaxy clusters Cygnus A, A3667, and A2065. Cygnus A appears to have a particularly simple merger geometry that allows an estimate of the subcluster collision velocity from the observed temperature variations. We estimate it to be $\sim 2000 \text{ km s}^{-1}$. Interestingly, this is similar to the free-fall velocity that the two Cygnus A subclusters should have achieved at the observed separation, suggesting that merger has been effective in dissipating the kinetic energy of gas halos into thermal energy, without channeling its major fraction elsewhere (e.g., into turbulence). In A3667, we may be observing a spatial lag between the shock front seen in the X-ray image and the corresponding rise of the electron temperature. A lag of the order of hundreds of kiloparsecs is possible due to the combination of thermal conduction and a finite electron-ion equilibration time. Forthcoming better spatial resolution data will allow a direct measurement of these phenomena in the cluster gas using such lags. A2065 has gas density peaks coincident with two central galaxies. A merger with the collision velocity estimated from the temperature map should have swept away such peaks if the subcluster total mass distributions had flat cores in the centers. The fact that the peaks have survived (or quickly reemerged) suggests that the gravitational potential also is strongly peaked. Finally, the observed specific entropy variations in A3667 and Cygnus A indicate that energy injection from a single major merger may be of the order of the full thermal energy of the gas. We hope that these order of magnitude estimates will encourage further work on hydrodynamic simulations, as well as more quantitative representation of the simulation results, in anticipation of the *Chandra* and *XMM* data.

Subject headings: cooling flows — dark matter — galaxies: clusters: individual (Cygnus A, A2065, A3667) — intergalactic medium — X-rays: galaxies

1. INTRODUCTION

Mergers of galaxy clusters are the most energetic events in the Universe since the Big Bang, with the total kinetic energy of the two colliding subclusters reaching 10^{63-64} ergs. In the course of a merger, a major portion of this energy, that carried by the subcluster gaseous halos, dissipates in the intracluster gas, heating it and possibly generating turbulence, magnetic fields, and relativistic particles. It is interesting to determine how much of this energy goes into turbulence and elsewhere, because this bears on the cosmologically important issue of the accuracy of the cluster total masses (e.g., Loeb & Mao 1994). A merger in a cooling flow cluster also subjects the cooling flow to ram pressure (e.g., McGlynn & Fabian 1984; Fabian & Daines 1991) and other destructive effects, directly probing the gas pressure and the depth of the gravitational potential in the cluster center. Detailed maps of mergers may also provide information on thermal conduction (and therefore magnetic fields) and electron-ion equilibration timescale in the intracluster plasma.

Merger shocks should produce strong spatial variations of the intracluster gas temperature and density (for a simulations review see, e.g., Burns 1998), such as those observed by *ASCA* and *ROSAT* in several dynamically active clusters (Henry & Briel 1995; Henriksen & Markevitch 1996; Honda et al. 1996; Donnelly et al. 1998, 1999; Churazov et al. 1999; Markevitch et al. 1994, 1996, 1998 [hereafter MFSV]). In this paper, we present the first temperature maps for three particularly interesting nearby merging clusters, Cygnus A, A3667, and A2065, obtained with *ASCA*. Despite the modest spatial resolution of

these maps, some qualitative conclusions regarding the physics of mergers and the shape of the cluster gravitational potential can be made. Unlike previous quantitative merger studies (e.g., Roettiger et al. 1998, 1999), we have chosen not to use the help of hydrodynamic simulations for the data interpretation, in order to examine what can be learned from a purely observational point of view. We use $H_0 = 50 \text{ km s}^{-1} \text{ Mpc}^{-1}$.

2. ASCA TEMPERATURE MAPS

ASCA (Tanaka et al. 1994) is capable of mapping the gas temperature in nearby clusters. MFSV analyzed Cygnus A, A2065 and A3667 as part of a larger *ASCA* cluster sample and presented average temperatures and radial temperature profiles for these clusters. The derivation of the projected gas temperature maps is described in detail in that paper and references therein. It involves the convolution of a two-dimensional temperature and emission measure model with the *ASCA* response, and fitting the temperatures in a number of spatial regions. As models for the emission measure, we used *ROSAT* PSPC images, taking into account the detected temperature variations. There is no PSPC image for A2065, so *Einstein* IPC and *ROSAT* HRI images were combined. The Cygnus A AGN spectrum was fitted simultaneously with all the gas temperatures as described in MFSV. The resulting gas temperature maps are shown in Figs. 1 and 3(b,c). Error estimates include all known calibration uncertainties. For the better-resolved Cygnus A and A3667, we also show maps of the gas specific (per particle) entropy, defined as $\Delta s \equiv s - s_0 = \frac{3}{2}k \ln [(T/T_0)(\rho/\rho_0)^{-2/3}]$, where the subscript 0 refers to any fiducial region in the cluster. For a qualitative

¹Harvard-Smithsonian Center for Astrophysics, 60 Garden St., Cambridge, MA 02138; maxim, alexey @head-cfa.harvard.edu

²Space Research Institute, Russian Academy of Sciences

³Astronomy Department, University of Virginia, Charlottesville, VA 22903; cls7i@virginia.edu

estimate, we approximate $\rho/\rho_0 \sim (S_x/S_{x0})^{1/2}$, where S_x is the cluster X-ray surface brightness in a given region.

All three clusters display significant gas temperature variations which, together with their complex X-ray brightness morphology, indicate ongoing mergers. Below we discuss some interesting implications for each cluster.

3. CYGNUS A

From the temperature and brightness maps, Cygnus A ($z = 0.057$) appears to have a particularly simple merger geometry, with two similar $T \simeq 4\text{--}5$ keV subclusters colliding head-on and developing a shock between them. Substructure is also observed in the optical (Owen et al. 1997). Taking advantage of this simplicity, we try to estimate the subcluster collision velocity directly from the observed gas temperature variations.

For such an estimate, we assume that the region between the Cygnus A subclusters can be approximated by a one-dimensional shock. Then following Landau & Lifshitz (1959) and using the Rankine–Hugoniot jump conditions, one can derive the difference of the gas flow velocities before and after the shock as a function of the respective gas temperatures:

$$u_0 - u_1 = \left[\frac{kT_0}{\mu m_p} (1-x) \left(\frac{1}{x} \frac{T_1}{T_0} - 1 \right) \right]^{1/2}, \quad (1)$$

where velocities are relative to the shock surface, indices 0 and 1 denote quantities before and after the shock ($0 < u_1 < u_0$ and $T_0 < T_1$), $\mu = 0.6$ is the plasma mean molecular weight, and

$$x \equiv \frac{u_1}{u_0} = \left[\frac{1}{4} \left(\frac{\gamma+1}{\gamma-1} \right)^2 \left(\frac{T_1}{T_0} - 1 \right)^2 + \frac{T_1}{T_0} \right]^{1/2} - \frac{1}{2} \frac{\gamma+1}{\gamma-1} \left(\frac{T_1}{T_0} - 1 \right). \quad (2)$$

The quantity x is the inverse of the shock compression, $x = (\rho_1/\rho_0)^{-1}$, and may also be determined from the increase in X-ray surface brightness at the shock as sometimes seen in X-ray images (e.g., Fig. 2 below). The application of these equations to the X-ray spectra assumes that the gas within the shocked region is nearly isothermal, and that electrons and ions reach equipartition. We will touch on these issues below.

For a symmetric merger in Cygnus A, we assume that the shocked gas on average is at rest relative to the center of mass. The collision velocity is then $\Delta u_{cl} = 2(u_0 - u_1)$. The pre-shock temperature can be estimated from the symmetric regions on the opposite sides of the subclusters, $T_0 \approx 4 \pm 1$ keV, and the post-shock value is $T_1 \approx 8_{-1}^{+2}$ keV (90% errors). The X-ray surface brightness in these regions is roughly consistent with the compression expected in the shock. Substituting these temperatures, we obtain $\Delta u_{cl} \approx 2200_{-500}^{+700}$ km/s.

Obviously, this simplistic shock model ignores many important details such as gas density gradients in subclusters, velocity and temperature gradients, and outflows along the shock plane. These effects are best taken into account by hydrodynamic simulations, as in, e.g., Roettiger et al. (1998, 1999). To gauge the importance of these effects, Ricker & Sarazin (1999) have simulated head-on cluster mergers similar to the one in Cygnus A. They find that there are significant temperature and velocity gradients within the shocked region which result from adiabatic compression, yet the simple shock velocity argument given above is accurate to about 20%.

Interestingly, the collision velocity found above is close to the free-fall velocity of ~ 2000 km s⁻¹ that two similar 4–5 keV,

$R \approx 1$ Mpc clusters should have achieved had they fallen from a large distance to the observed separation of 1 Mpc. This consistency may suggest that kinetic energy of the gas in colliding subclusters is effectively thermalized, since otherwise (e.g., if a major fraction of this energy were channeled into turbulence, magnetic fields, or cosmic rays) the shock temperature would not be as high as observed.⁴

4. A3667

A3667 is a spectacular merger at $z = 0.053$. It also has an extensive double radio halo outside the central region (Röttgering et al. 1997), straddling our region of measured temperatures as shown in Fig. 1. The galaxy distribution is bimodal (Proust et al. 1988), with the main component around the cD galaxy in region 5 of Fig. 1 and the secondary component around the second-brightest galaxy in region 14. The hottest gas is observed between these subclusters, indicating that they are presently colliding (although not necessarily for the first time). The brightness peak seems to lag behind the cD galaxy (Fig. 1), consistent with this picture. The merger is apparently more complex than in Cygnus-A, but for order of magnitude estimates, we still apply the simple modeling of §3. For pre- and post-shock temperatures of 4 keV and 10 keV, the collision velocity is likely to be of the order of $2(u_0 - u_1) \sim 2500\text{--}3000$ km s⁻¹, and the velocities of the two shocks propagating from the site of the collision in region 10 of the map are $u_1 \sim 1000$ km s⁻¹ relative to the collision site.

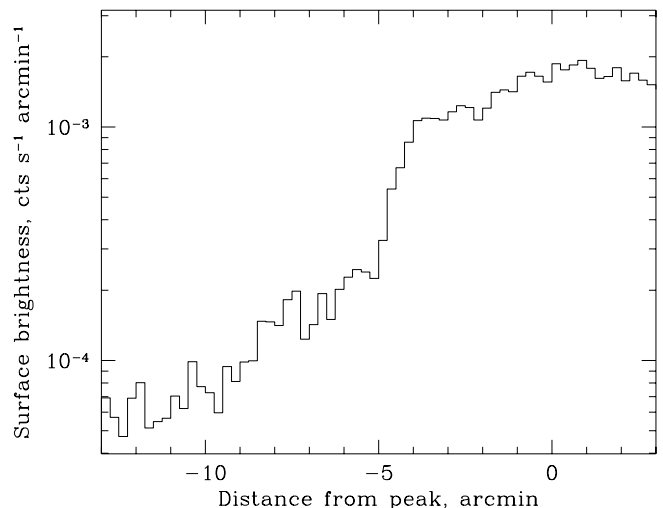


FIG. 2.—A3667 *ROSAT* PSPC linear brightness profile in a 3'-wide strip along the direction of the cluster elongation (from region 2 to region 8 in Fig. 1). A shock front is apparent at $-5'$ from the brightness peak, inside region 2 of the temperature map. A similar feature is present in the HRI image.

The *ROSAT* image suggests that one of these shock fronts has reached region 2 of our map (Fig. 2). We do not see an accompanying high temperature there, while we do observe an elevated temperature at the collision site. It is quite possible that measurement errors and projection effects have reduced the temperature rise. There is also a more interesting but rather speculative explanation: that there is a spatial lag

⁴Note, however, that such a consistency by itself cannot prove that in general there are no dynamically important turbulence or magnetic fields in clusters, since for the free-fall velocity calculation, masses are estimated from the gas temperature assuming the absence of such effects.

between the gas density jump and the corresponding electron temperature increase due to the lack of equipartition between electrons and ions at the shock front and/or due to the effects of thermal conduction (Shafranov 1957). It is unclear to what extent electrons will be dissipatively heated in the moderate Mach number collisionless shocks in cluster mergers. If the electrons are not heated dissipatively, it takes about $t_{ep} \simeq 2 \times 10^8 \text{ yr } (n_e/10^{-3} \text{ cm}^{-3})^{-1} (T_e/10^8 \text{ K})^{3/2}$ for the temperatures to equilibrate through electron-proton collisions (Spitzer 1962). During this time, a 1000 km s^{-1} shock will travel ~ 0.2 Mpc. Electrons will also be heated by adiabatic compression in the shock, and this process is more important in weaker shocks, such as those in mergers. For the crude estimate of the shock parameters given above, the compression is $\rho_1/\rho_0 \approx 2.5$, consistent with the increase in X-ray brightness in Fig. 2. This implies an adiabatic increase in the electron temperature by a factor of ~ 1.9 . It is possible that electron thermal conduction, if not strongly suppressed, will act to smooth out this electron temperature jump. Given the present crude temperature information and the uncertainty of the merger stage, this discussion is very speculative. However, future observations with *Chandra* might provide much more detailed electron temperature and gas density profiles in merger shocks in A3667 and other clusters. This would allow a direct study of electron heating, thermal conduction (and therefore magnetic fields), and the rates of electron-ion equipartition in the intracluster gas. In the meantime, our estimates indicate the need to include these observable effects in the hydrodynamic merger simulations. Indeed, simulations by Takizawa (1999) exhibit qualitatively similar deviations of T_e from the plasma mean temperature at a late merger stage.

Assuming that, in general, T_e represents the local mean temperature reasonably well, it is interesting to note that specific entropy maps of A3667 and Cygnus A (Fig. 1) show variations of the order of $\frac{3}{2}k$. Energy that needs to be injected into the gas to produce such entropy changes is $Q \simeq T \Delta s$. Therefore, such variations indicate that energy input from the merger is comparable to the gas thermal energy, $\frac{3}{2}kT$, providing direct empirical evidence that mergers at the present time can contribute significantly to the heating of the intracluster gas.

5. A2065

The temperature map of A2065 ($z = 0.072$) reveals a hot region southeast of the cluster peak which is probably a merger shock. The elongated galaxy distribution in the inner $r \sim 10'$ (Postman, Geller, & Huchra 1988) is rather similar to the X-ray contours and does not show any distinct subclusters. This suggests that the merger is at a late stage, perhaps well after a core passage, although the data are too crude to discuss any definitive scenarios. There is a marginally significant spectroscopic indication of a mild cooling flow in the center (MFSV). Using a *ROSAT* HRI image, Peres et al. (1998) estimate a central cooling time of ~ 4.4 Gyr and $\dot{M} = 13^{+14}_{-6} M_\odot \text{ yr}^{-1}$. Overlaying the *ROSAT* HRI image onto a Digitized Sky Survey plate (Fig. 3a) reveals two peaks in the X-ray brightness, coincident with two central galaxies with a projected separation of ~ 35 kpc (whose line of sight velocities differ by $\sim 600 \text{ km s}^{-1}$; Postman et al. 1988). It is remarkable that these peaks have survived a merger. We will use their survival to constrain the compactness of the gravitational potential at the subcluster centers.

Many if not most clusters have sharp central gas density peaks due to the cooling flows (e.g., Peres et al. 1998). Because of the spectral complexity of these regions, it is unclear if

the gas pressure also is peaked, as it would be if the dark matter distribution has a central cusp (e.g., Navarro, Frenk, & White 1995). Alternatively, the central temperature drop might keep the pressure gradient low, as required for a dark matter distribution with a flat core such as a King profile. *ASCA* spectral analyses of stationary cooling flows, although somewhat uncertain, indicate the presence of a hot gas phase, supporting the first possibility (e.g., Fukazawa et al. 1994; Ikebe et al. 1996), which is also consistent with strong gravitational lensing results (Allen 1998). A merger in a cooling flow cluster can provide an independent probe of the central gas pressure, including its hypothetical nonthermal component (e.g., Loeb & Mao 1994) inaccessible by the spectral analysis.

Whether the two central galaxies in A2065 are physically interacting or a chance projection is not obvious from the optical data. If these galaxies are at the centers of the colliding subclusters and are physically close then both should have experienced the full effect of a merger sweeping the collisional gas away from the collisionless galaxies and dark matter peaks (while the latter would likely survive; e.g., González-Casado et al. 1994). On the other hand, if they are separated along the line of sight then it seems unlikely that both have avoided the shock passage. We assume for definiteness that the shock in region 2 has passed over the southern galaxy, although of course, this is not the only scenario.

This leads to two possibilities, that the observed gas density peak around the galaxy (whether due to a cooling flow or not) has survived the shock, or it has reestablished itself after the shock passage. Again neglecting the uncertain merger geometry and stage for a qualitative estimate, from the observed temperature variations $T_0 \simeq 5$ keV and $T_1 \simeq 14$ keV and eqs. (1) and (2), one estimates $u_0 - u_1 \simeq 1800 \text{ km s}^{-1}$. Given this velocity scale, the time since a shock may have passed the cluster center is of order a few $\times 10^8$ yr, much shorter than the central cooling time of 4.4 Gyr (Peres et al. 1998). Thus, if the hot gas has settled in the gravitational potential after the shock passage, it should still be hot and therefore, its peaked density distribution must reflect a peak of the gravitational potential.

On the other hand, if this density peak has survived the shock passage intact, then its gas pressure must be greater than the ram pressure of the gas flowing around the peak, $p_{\text{peak}} \gtrsim p_{\text{ram}} \sim \rho'(u_0 - u_1)^2$ (e.g., Daines & Fabian 1991). As a rough estimate of the density of the gas exerting ram pressure, ρ' , we take the average density of the central region of A2065, found by fitting a β -model to the HRI brightness profile centered on the global cluster emission centroid, which is slightly offset from the peak. We use the average temperature of 5.5 keV and the cluster region inside 1.6 Mpc, simultaneously fitting the constant HRI background. For this fit, we obtain $a'_x = 150$ kpc, $\beta' = 0.49$, $n'_{H0} = 5 \times 10^{-3} \text{ cm}^{-3}$ and $\rho' = 1.2 \times 10^{-26} \text{ g cm}^{-3}$, resulting in the estimate $p_{\text{peak}} \gtrsim 4 \times 10^{-10} \text{ erg cm}^{-3}$. We can similarly estimate the gas density in the peak, fitting a β -model to the brightness profile centered exactly on the southern galaxy and using only the southern half of the cluster image to exclude the brightness extension on the opposite cluster side. Although the profile does not follow the β -model in the very center, it is still a convenient representation for our purpose. The fit gives $a_x = 50$ kpc, $\beta = 0.42$ and $n_{H0} = 1.2 \times 10^{-2} \text{ cm}^{-3}$. With this n_{H0} , the peak pressure estimated above corresponds to a temperature $T_{\text{peak}} \gtrsim 9$ keV, compared to the cluster average temperature of 5.5 keV. The *ASCA* measurement in region 1 of Fig. 3b, although uncertain, does not exclude the existence of such a hot

gas. Note, however, that the above high pressure need not necessarily be of thermal nature.

We can now estimate the total mass around the southern galaxy using the above pressure constraint. For a rough estimate we assume that $p(r) \propto \rho_{\text{gas}}(r)$ (which corresponds to isothermal gas if the pressure is thermal), that the gas is not far from hydrostatic equilibrium, and substitute the above β -model parameters for the peak density distribution to the hydrostatic equilibrium equation $dp/dr = -\rho_{\text{gas}}GM(r)/r^2$ (e.g., Sarazin 1988). For example, within $r = a_x = 50$ kpc we obtain $M \gtrsim 1.1 \times 10^{13} M_{\odot}$. For comparison, if one uses the average cluster temperature of 5.5 keV and the gas density parameters of the centroid fit α'_x and β' obtained above, thereby assuming that the density peaks on the galaxies are due solely to the isobaric cooling flows, one obtains a 7 times lower mass within the same radius. Thus, the survival of the gas density concentration centered on one of the giant central galaxies indicates that there indeed is a sharp pressure peak at that position, implying a sharply peaked total mass profile with the galaxy at the peak. Note that the estimated mass in the peak is too great to be due to the galaxy itself ($M/L_B \gtrsim 100 M_{\odot}/L_{\odot}$, photometry from Postman et al. 1988).

6. SUMMARY

Using *ASCA*, *ROSAT* and *Einstein* data, we derived gas temperature maps of Cygnus A, A3667, and A2065. The maps

indicate ongoing major mergers and allow us to make several interesting qualitative estimates. (1) The observed temperature variations in Cygnus A are close to those expected for a free-fall collision of two subclusters with Cygnus A masses, suggesting that the gas kinetic energy is effectively dissipated into heat during a merger. (2) In A3667, we may be observing a spatial lag between the shock front seen in the *ROSAT* images and the rise of the electron temperature. A considerable lag might be produced by the finite electron-ion temperature equilibration time and the effects of thermal conduction. (3) In A2065, the double gas density peak centered on two central galaxies apparently has survived a merger shock passage. From this, we infer a lower limit on the total pressure in the peak which implies a strongly peaked total mass distribution. (4) Specific entropy variations in A3667 and Cygnus A provide direct empirical evidence that present-day major mergers contribute significantly to the heating of the intracluster gas. Data from *Chandra*, *XMM*, and *Astro-E*, together with improved simulations, will allow much deeper insights into the physics of cluster mergers.

We thank Marc Postman for providing his A2065 optical image prior to publication, and the referee for many useful comments. Support was provided by NASA contracts NAS8-39073, NAG5-3057, NAG5-4516, and CfA postdoctoral fellowship.

REFERENCES

- Allen, S. W. 1998, *MNRAS*, 296, 392
 Burns, J. O. 1998, *Science*, 280, 345
 Churazov, E., Gilfanov, M., Forman, W., & Jones, C. 1999, *ApJ*, in press
 Donnelly, R. H., Markevitch, M., Forman, W., Jones, C., Churazov, E., & Gilfanov, M. 1999, *ApJ*, in press
 Donnelly, R. H., Markevitch, M., Forman, W., Jones, C., David, L. P., Churazov, E., & Gilfanov, M. 1998, *ApJ*, 500, 138
 Fabian, A. C., & Daines, S. J. 1991, *MNRAS*, 252, 17p
 Gonzalez-Casado, G., Mamon, G. A., & Salvador-Solé, E. 1994, *ApJ*, 433, L61
 Fukazawa, Y., et al. 1994, *PASJ*, 46, L55
 Henriksen, M., & Markevitch, M. 1996, *ApJ*, 466, L79
 Henry, J. P., & Briel, U. G. 1995, *ApJ*, 443, L9
 Honda, H., et al. 1996, *ApJ*, 473, L71
 Ikebe, Y., et al. 1996, *Nature*, 379, 427
 Landau, L. D., & Lifshitz, E. M. 1959, *Fluid Mechanics* (London: Pergamon), §§ 82,85
 Loeb, A., & Mao, S. 1994, *ApJ*, 435, L109
 Markevitch, M., Forman, W. R., Sarazin, C. L., & Vikhlinin, A. 1998, *ApJ*, 503, 77 (MFSV)
 Markevitch, M., Sarazin, C. L., & Irwin, J. A. 1996, *ApJ*, 472, L17
 Markevitch, M., Yamashita, K., Furuzawa, A., & Tawara, Y. 1994, *ApJ*, 436, L71
 McGlynn, T. A., & Fabian, A. C. 1984, *MNRAS*, 208, 709
 Navarro, J. F., Frenk, C. S., & White, S. D. M. 1995, *MNRAS*, 275, 720
 Owen, F. N., Ledlow, M. J., Morrison, G. E., & Hill, J. M. 1997, *ApJ* 488, L15
 Peres, C. B., Fabian, A. C., Edge, A. C., Allen, S. W., Johnstone, R. M., & White, D. A. 1998, *MNRAS*, 298, 416
 Postman, M., Geller, M. J., & Huchra, J. P. 1988, *AJ*, 95, 267
 Proust, D., Mazure, A., Sodré, L., Capelato, H. V., & Lund, G. 1988, *A&AS*, 72, 415
 Ricker, P., & Sarazin, C. L. 1999, in preparation
 Roettiger, K., Stone, J. M., & Mushotzky, R. F. 1998, *ApJ*, 493, 62
 Roettiger, K., Burns, J. O., & Stone, J. M. 1999, *ApJ*, in press
 Röttgering, H. J. A., Wieringa, M. H., Hunstead, R. W., & Ekers, R. D. 1997, *MNRAS*, 290, 577
 Sarazin, C. L. 1988, *X-ray Emission from Clusters of Galaxies* (Cambridge: Cambridge University Press)
 Shafranov, V. D. 1957, *Soviet Phys. JETP*, 5, 1183
 Spitzer, L. 1962, *Physics of Fully Ionized Gases* (New York: Wiley)
 Takizawa, M. 1999, *ApJ* in press
 Tanaka, Y., Inoue, H., & Holt, S. S. 1994, *PASJ*, 46, L37

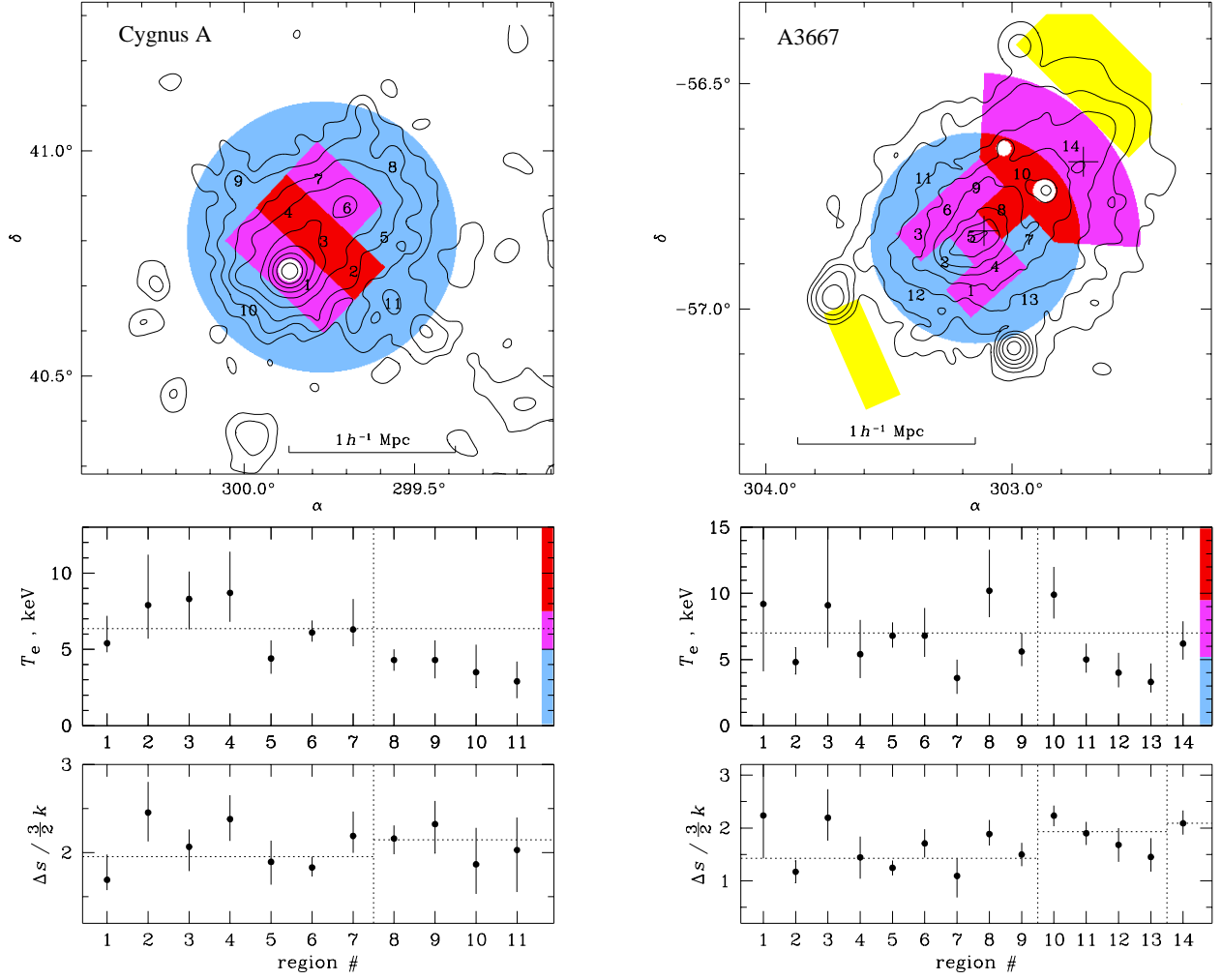


FIG. 1.—ASCA projected temperature maps (color) overlaid on the *ROSAT* PSPC brightness contours spaced by a factor of 2. Regions in which the temperature was derived are numbered in upper panels; their temperatures and specific entropies with 90% errors are given in lower panels, along with the color scale for the temperature. Different colors correspond to significantly different temperatures. Dotted vertical lines separate groups of regions belonging to the same annulus or a central square. Dotted horizontal lines show temperature averaged over the cluster or entropy averaged over the respective annulus or square. White circles in the maps show point sources either excluded or fitted separately (some are not shown for clarity). Region 1 in Cygnus A is a $6' \times 18'$ rectangle with the AGN region excised. For A3667, crosses mark positions of the two brightest galaxies, and yellow areas schematically show the radio halo from Röttgering et al. 1997).

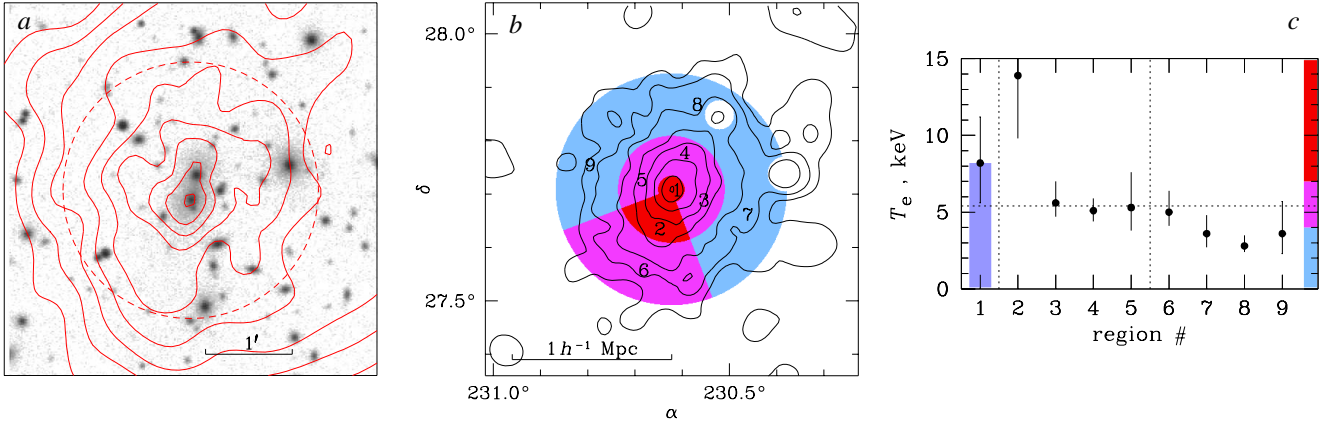


FIG. 3.—(a) *ROSAT* HRI image of the central region of A2065 (contours) overlaid on the Digitized Sky Survey image. The contours are spaced by a factor of $\sqrt{2}$. An $8''$ correction was applied to the HRI coordinates using two point sources in the field of view. Dashed circle of $r = 1.5'$ corresponds to region 1 in panel (b), which shows ASCA temperature map (colors) overlaid on the *Einstein* IPC brightness contours (spaced by a factor of 2). Regions are numbered and their temperatures with 90% errors are shown in panel (c). For region 1, ambient temperature of a cooling flow is shown and blue band denotes the cooling flow.